Detailed and simplified models of bolted joints under impact loading

N Tanlak[1], **FO Sonmez**[1]*, and **E Talay**[2]
[1]Department of Mechanical Engineering, Bogazici University, Istanbul, Bebek 34342, Turkey
[2]TOFAS Turk Otomobil Fabrikasi, Bursa, 16369, Turkey

The manuscript was received on 21 October 2010 and was accepted after revision for publication on 16 December 2010.

DOI: 10.1177/0309324710396997

Abstract: Mechanical components are commonly fastened together using bolts. In many applications, they are subjected to impact loads during their service life. Their response and failure behaviour under these conditions needs to be known for their safe use. The objective of this study was to develop computationally efficient and accurate finite element models for bolted joints under impact loading. First, a three-dimensional detailed finite element model for a bolted joint was developed using solid elements. With this full modelling, the aim was to simulate the physics of the impact event as accurately as possible without any concern about computational cost. In the design of mechanical structures containing numerous fastening elements, use of detailed models is not practicable, because the computational cost of the analysis dramatically increases with the increased number of complex interacting parts. Instead, simplified models that only account for dominating effects should be utilized so that the analysis time can be significantly reduced without compromising the level of accuracy. Accordingly, a number of simplified finite element bolt models were developed and then compared with the full model with regard to the solution accuracy and computational cost to select the most representative and cost-effective simplified model.

Keywords: bolted lap joints, crash, explicit finite element analysis, simplified models

1 INTRODUCTION

Bolts are one of the most commonly used fastening elements in the assembly of mechanical parts. They are used in almost every engineering application. Structures with bolted joints are usually subjected not only to various static loads but also to impact loads. Because bolts provide localized connection, they lead to high stress concentration in the joined plates. Considering that impact loads are much more damaging at notches, the region around a bolt is one of the most critical locations in the plates. Designing for safety requires accurate determination of stress and strain states in the critical locations so that damage done during a crash can be predicted.

A bolted joint by itself is a very complex part considering the complexity of its geometry, the contact between teeth of the bolt and the nut, the pre-tension in the bolt shank, contact surfaces between the nut and the washer, bolt head and the washer, washers and the sheets, bolt shank and the holes of the sheets. Although very complex phenomena can be simulated with today's computational capabilities and commercial finite element codes, proper decisions need to be made regarding the constitutive model, the model of the material, element type, mesh structure, step size, etc. to produce an accurate representation of a physical event. Another difficulty is that given the complexity of a single bolted joint, analysis of panels or beams fastened by many bolts is quite a demanding and time-consuming task. If one tries to simulate the behaviour of such a structure with all its complexity, the results cannot be obtained within a time short enough to be of use in a design process, which requires trials of many configurations to find an effective design. For this reason, the complex geometry should be simplified so as to reduce the computational burden without compromising accuracy.

*Corresponding author: Department of Mechanical Engineering, Bogazici University, Istanbul, Bebek 34342, Turkey.
email: sonmezfa@boun.edu.tr

The literature on bolted joints is significantly biased towards the consideration of static loadings [**1**–**15**]. Mistakidis and Baniotopoulos [**1**] used plane stress elements to model bolted joints without considering the pre-tension in the bolt. The thickness of the plane stress elements was chosen such that it was possible to account for the effects of the three-dimensional features of the structure. Most papers in the literature simulate the behaviour of the bolt–nut assembly using three-dimensional solid elements in order for the model to be as realistic as possible [**2**–**12**, **15**]. In some studies [**3**, **4**, **16**], the bolt shank as well as bolt head are modelled using beam elements. Barth *et al.* [**9**] and Webber *et al.* [**13**] assumed the bolts to be rigid. Butterworth [**14**] modelled the nut and head of the bolt using brick elements and the bolt shank with a beam element. Except for the notable exception of Kishi *et al.* [**7**], generally, the nut and bolt head are modelled as being cylindrical rather than hexagonal to simplify the geometry. Chung and Ip [**5**, **6**] introduced a small artificial hole through the central axis of the bolt for ease of meshing; the hole being small enough not to affect the behaviour of the joint. Some studies [**7**–**12**, **16**] have used a clamping force obtained via a prescribed displacement to account for the pre-tension in the bolt. Citipitioglu *et al.* [**10**] induced the pre-tension in two steps: first, the length of the bolt was specified to be shorter than the total thickness of the joined plates and a prescribed displacement was then imposed on the bolt. In the second step, the contact between the displaced bolt head and its respective surface was activated and the imposed displacement was released. McCarthy *et al.* [**15**] defined an artificial thermal expansion coefficient for one of the washers. By introducing a temperature difference, the resulting expansion in the washer caused a pre-tension in the bolt.

In comparison to the literature on static loading, papers that discuss bolted joints subjected to dynamic loads are rare [**16**–**20**]. Sabuwala *et al.* [**18**] analysed bolted joints under blast and cyclic loads. The bolt and the nut were modelled as separate parts contrary to the prevailing custom in which the nuts are considered to be an integral part of the bolts. Reid and Hiser [**19**] modelled the nut and the head of the bolt as having a hexagonal shape and included the washers in their analysis. They analysed the cases in which the bolt was either rigid or could be deformed. Kim *et al.* [**16**] used various simplified bolt models to find the natural frequency of the structure. They introduced artificial coefficients of thermal expansion for the bolt shank to induce the pre-tension. Oldfield *et al.* [**20**] induced the pre-tension of the bolt by using an implicit solver, then imported the results to the explicit solver, and analysed the structure under cyclic loading via the explicit solver in order to reduce the computational time. Kwon *et al.* [**17**] introduced both a three-dimensional detailed bolt model and some simplified bolt models. In one of the simplified models, the bolt head and the nut were modelled with shell elements, whereas the shank of the bolt was modelled with solid elements. In another simplified model, the entire bolt–nut assembly was modelled with shell elements. Hendricks and Wekezer [**21**] proposed two different simplified finite element models for the bolted connection of guardrails. In an alternative simplified model, they used tie constraints. O'Daniel *et al.* [**22**] used connecting beam elements through the mesh of the panels in order to simulate the behaviour of the bolted joints.

These published studies are overwhelmingly concerned with bolted joints under static loading with only a few studies having considered impact loads. Although some simplified models have been proposed for both static and impact loads, they have not been evaluated for computational efficiency and accuracy of the predicted stress and strain states under high loads causing plastic deformation. Also, they do not focus on the region around the bolt holes, although this is one of the most critical regions in sheets fastened by bolts.

2 PROBLEM STATEMENT

In automotive applications, usually thin panels are used that are joined by bolts or spot welds. For this reason, the panels themselves are expected to fail, but not the bolts. Failure generally occurs at the point of an impact on the panel or around the bolts. Thus, finite element models of bolted joints should correctly estimate the plastic strains around the bolt holes in order to be able to predict their failure.

Other concerns are the computational efficiency and difficulty of the modelling procedure. A detailed model of a bolted joint that accounts for all aspects of the physics of the problem requires the consideration of many geometric details and many contact relations between different parts of the joint. Considering that even a simple panel may contain many fasteners, analysing the structure with all its complexity leads to excessively long computational times. In addition the designer also needs to devote considerable time to the modelling of the complex

geometry. This combination renders the use of a full model impracticable in typical applications in engineering design. Thus, there is a need for a finite element model of bolted joints that reduces the complexity of the geometry and the number of contact relations so that the analysis can be completed in a relatively short time without significantly compromising the accuracy.

This study considers bolted joints under high impact loads that induce large plastic strains in the sheets and focuses on correctly determining the strain state around the bolt holes and at the same time developing computationally efficient simplified models.

3 APPROACH

In order to reduce the computational time and modelling difficulty, simplified models were developed for the analysis of bolted joints subjected to impact loads. The simplified models reflect only the effects of the dominant factors on the behaviour of bolted joints in holding the plates together and transmitting the forces between the plates. Accordingly, the number of interacting components is reduced in these models, and also many geometric details are omitted. In the absence of experimental data, a detailed model was developed in order to validate the simplified models through a comparison of their results. The detailed bolt model reflects almost all aspects of the physics of the problem: including all the contact relations, most of the geometric details, and the pre-tension in the bolt shank. This model is used as a benchmark for the computational cost and accuracy of the simplified models.

Under impact loadings, structures are usually analysed via explicit finite element codes because they are better suited to the analysis of structures involving complex contact interactions and large deformation [**23**]. Accordingly, a commercial finite element analysis software based on explicit formulations, ABAQUS/Explicit, was used in this study.

4 DETAILED FINITE ELEMENT MODELLING OF BOLTED JOINTS: FULL MODEL

The objective of this model is to obtain accurate results regardless of the computational burden incurred in its solution. For this reason, the bolt model is made as detailed as possible. Nevertheless, some features of the geometry that are assumed to have insignificant effect on the response of the joint are ignored. First, the threads of the bolt and the nut are omitted and the bolt–nut assembly is modelled as a monolithic structure assuming that relative motion between bolt and nut, or loosening, does not take place during impact. In other words, the nut is an integral part of the bolt. Second, the bolt head and the nut are modelled as being cylindrical rather than hexagonal since the pressure on the sheets is directly applied by the washers and the meshing of hexagonal shapes with uniform finite elements is difficult. Lastly, the chamfers and the fillets of the bolt are neglected. The other features of the geometry are taken into account in the model. The washers are modelled separately. All of the components are taken to be deformable.

It should be noted that because the sheets are assumed to be the most critical element, this study focuses not on the bolt but instead on how the stress and strain states in the sheets can be accurately determined. The modifications in the bolt and the nut are assumed not to cause error in the calculated values of stress in the sheets because they do not affect the stiffness properties of the bolt–nut assembly; however, removing teeth and fillet, i.e. omitting notches under impact loading, certainly leads to erroneous results for the bolt.

4.1 Model geometry of the joined sheets

In this study, a drop test is simulated as depicted in Fig. 1. A sheet of material called the ‘plate’ is fastened by a single bolt at each end to a thicker sheet called the ‘frame’, which is in turn fixed to the main frame. The plate is hit at the middle by an impactor dropped from a certain height. Benefiting from the symmetry of the structure, only half of it needs to be analysed. Figure 2 shows the individual components. The dimensions of the plate and the frame are $1\times32\times130$ and $2\times32\times22$ mm, respectively. The hole has a radius of 4.2 mm; its centre is 11 mm away from the fixed end. The washers have a thickness of 1 mm. Their inner and outer radii are 4.5 and 8.5 mm, respectively. The bolt has typical dimensions of M8 type. Namely, its shank has a diameter of 8 mm, the bolt head and nut have a diameter of 14 mm, and a thickness of 5.6 mm.

4.2 Material model

The mechanical behaviour of materials under impact loading depends on the strain rate. With increased strain rates, materials commonly exhibit

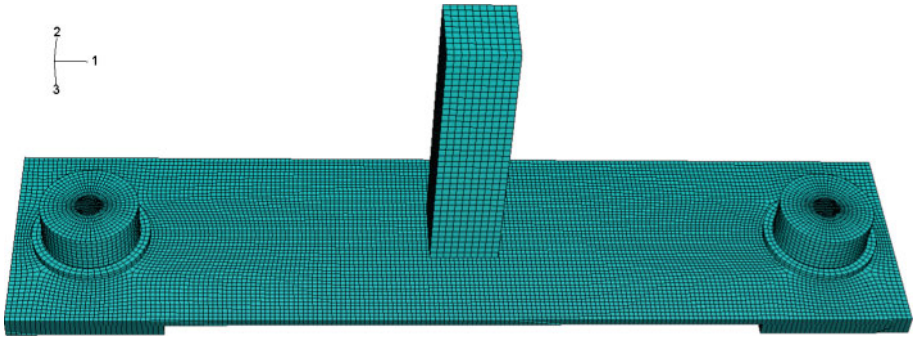

Fig. 1 The full model for a drop test

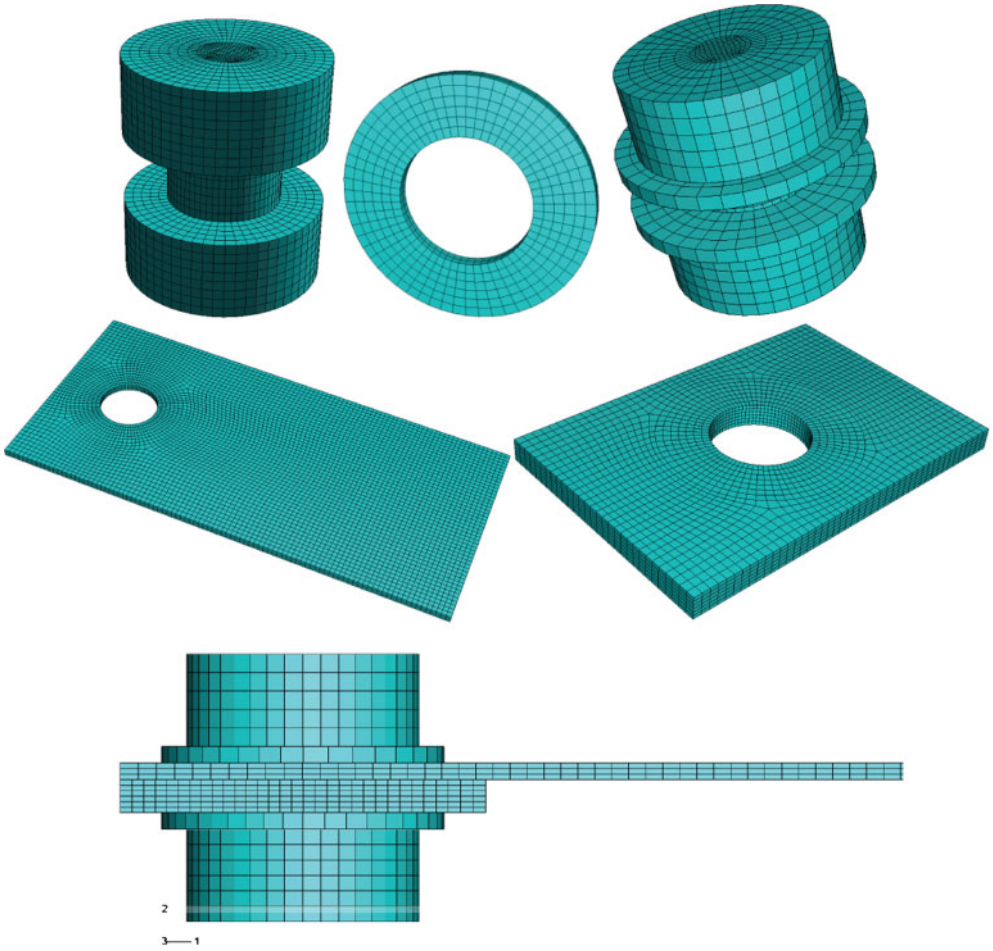

Fig. 2 The individual components of the symmetric half model

an increase in their yield strengths. The sheets considered in this study are made of steel. Strain-rate-dependent stress–strain relations determined experimentally for this material are used in the simulation. The data were provided for strain rates between 0.1 m/m.s, i.e. under quasi-static condition, and 500.00 m/m.s as shown in Fig. 3. The material has an elastic modulus of 205 GPa, a Poisson's ratio of 0.33, and a density of 7800 kg/m^3. An isotropic hardening model was used in the finite element model simulations, with the size of the yielded region changing uniformly in all directions.

The impactor is assumed to be elastically deformed. It has an elastic modulus of 600 GPa, a Poisson's ratio of 0.3, and density of 30 000 kg/m^3. Additionally, the bolt and washer material has an

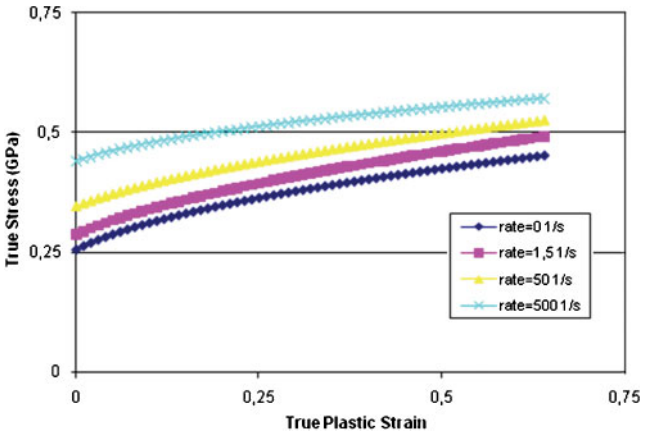

Fig. 3 The true stress–strain curve of the material under different strain rates in the plastic region

elastic modulus of 210 GPa, a Poisson's ratio of 0.3, and a yield strength of 240 MPa.

4.3 Meshing

A suitable type of element needs to be selected for the finite element model to obtain reliable results. First, the element should have large strain and large deflection capabilities in order to account for the large deformations experienced by the structure during impact. Second, because the full model should be based on the three-dimensional geometry of the bolted joint, the element types should be compatible with it. Third, the element should allow reduced integration for computational effectiveness. Because reduced-integration elements do not create stiffness in some deformation modes, an unstable motion, called hourglassing, may occur. By taking all these considerations into account, eight-node linear brick elements (C3D8R) with reduced integration and hourglass control are used to generate the finite element mesh for the solid models of the frame, the plate, bolt–nut, and the washers (Fig. 2).

4.4 Boundary conditions

The boundary conditions defined on the model should realistically reflect the loading conditions on the structure. All degrees of freedom are restrained on one side of the frame and symmetry conditions are specified on the plate on the symmetry plane. The impactor has a length of 40 mm and a square cross-section of 10×10 mm. A half of it is modelled with symmetry conditions defined on the cutting plane. The joint and the impactor are subjected to a gravitational field of 9.81 m/s^2 in the negative direction of axis 2. The velocity of the impactor is 25 m/s at the instant of impact.

4.5 Pre-tension in the bolt

In order to take into account the effect of the pre-tension in the bolt shank, an artificial anisotropic coefficient of thermal expansion is defined for one of the washers. A temperature increase induces expansion of the washer only in the axial direction, which in turn induces tension in the bolt shank and compression in the clamped members.

4.6 Contact conditions

One of the key issues in the analysis of bolted joints is how to simulate the interacting components. In this study, the contact between the plate and the impactor is modelled by a finite-sliding contact with a penalty contact algorithm rather than a kinematic contact enforcement method. The reason for this choice is that the contact conditions at the joint cannot be modelled using the kinematic contact algorithm in some simplified models. For consistency and comparability, the penalty contact algorithm is used to enforce the contact between the contacting surfaces in all the models.

Contacting surfaces in the joint have almost identical meshes. This helps to improve the analysis time. Ten contact pairs are created in the detailed finite element model as follows.

1. Contact pair 1: the bottom surface of the impactor and the region on the top surface of the plate hit by the impactor.
2. Contact pair 2: the bottom surface of the plate and the top surface of the frame.
3. Contact pair 3: the bottom surface of the head of the bolt and the top surface of the corresponding washer.
4. Contact pair 4: the top surface of the plate and the bottom surface of the corresponding washer.
5. Contact pair 5: the bottom surface of the frame and the top surface of the corresponding washer.
6. Contact pair 6: the top surface of the nut and the bottom surface of the corresponding washer.
7. Contact pairs 7 and 8: the surface of the bolt shank and the inner surfaces of the washers.
8. Contact pairs 9 and 10: the surface of the bolt shank and the inner surfaces of the bolt holes in the plate and the frame.

4.7 Friction model

When in contact, solid bodies usually transmit normal as well as shear forces across their interface. Generally, a relationship exists between these two force components. The relationship depends on the

magnitude of the contact forces as well as slip rate. In this study, a Coulomb friction model is adopted. Typical values are chosen for static and kinetic friction coefficients in metal-to-metal contact, which are 0.15 and 0.12, respectively. To create the transition from a zero slip rate to high slip rates, an exponentially decaying function is used for the frictional coefficient.

4.8 Time increments

The time increment used in an explicit analysis should be smaller than the stability limit of the central-difference operation. Otherwise, the solution becomes unstable and displacements may oscillate with increasing amplitudes. The stability limit is usually chosen as the smallest transition time of a stress wave across any element in the mesh. In crash problems involving large deformations, the highest frequency of the model varies during impact, which consequently alters the stability limit. For this reason, a fully automatic time-increment scheme in ABAQUS/Explicit is used in the present analyses to account for changes in the stability limit.

5 SIMPLIFIED FINITE ELEMENT MODELS

In this study, a number of models were developed to simulate the clamping effect of bolted joints in a simplifying manner by accounting for only the dominant factors. All the simplified models were then compared with the full model regarding accuracy and computational time. In order to reach a meaningful comparison, almost all the parameters and analysis options including mesh pattern and contact enforcement methods were chosen to be the same in all the models.

In the simplified models, shell elements are used instead of solid elements to model the metal sheets based on the fact that the thickness is very small in comparison to the lateral lengths. The element type used in the models is S4R, a four-node quadrilateral shell element which resulted in a reduced number of integrations and a large-strain formulation. Simpson's integration rule is used with five integration points through the thickness.

5.1 Simplified model 1: full model with shell plates

In this model, the model for the bolt–nut assembly is the same as the detailed model; but the plate and the frame are discretized using shell elements (Fig. 4) considering that their thickness-to-lateral length ratio is less than 1/10. The shells are positioned at the mid-surface of the sheets. The same contact pairs as in the full model are defined.

5.2 Simplified model 2: rigid shank with coupling constraints

In this model, the bolt shaft is conceived as a smooth cylindrical shaft discretized with solid elements (Fig. 5). It is taken to be rigid on the basis that it is considerably more stiff than the sheet because of its large diameter in comparison to the sheet's thickness. The effects of the bolt head and nut are simulated through coupling constraints. The central nodes on the upper and lower surfaces of the cylinder are used as control points for the coupling constraints. The constraints are applied to the surfaces of the sheets that are under the direct clamping pressure of the washers. A distributing coupling constraint is used in which all degrees of

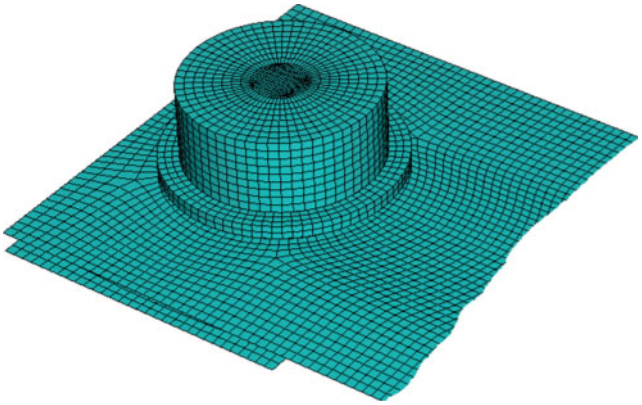

Fig. 4 Simplified model 1: full model with shell plates

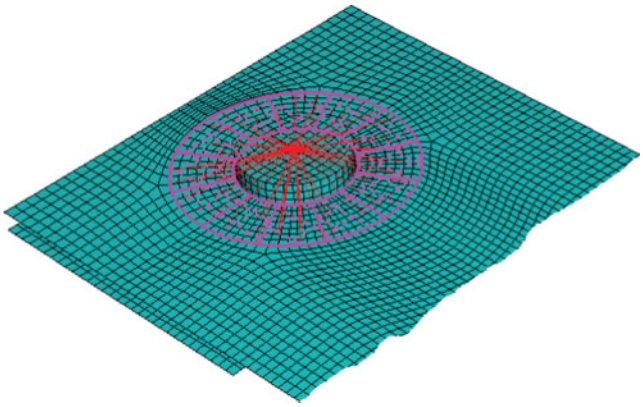

Fig. 5 Simplified model 2: rigid shank with coupling constraints

freedom are restrained. In this way, the relative motion between the ends of the bolt shank and the compressed region on the sheets is prevented. This means that the bolt head, nut, and washers are assumed to be non-deformable and relative motion between the washers and the sheets is assumed not to exist. Only the contact pairs 1, 2, 9, and 10 are introduced in this model.

5.3 Simplified model 3: deformable shell bolt

In this model, the bolt–nut assembly is modelled using shell elements. The geometry and mesh structure are shown in Fig. 6. The flat portions of the model simulate the restrictive effect of the washers. In this model, the shell has a thickness of 1 mm. In order to make the bending stiffness of the cylindrical shell equal to that of the bolt shank, the product of the elastic modulus and moment of inertia, EI, is made the same as that of the bolt shank. Then, from

$$E_c = E_b I_b / I_c \tag{1}$$

the elastic modulus of the material of the cylindrical shell, E_c, is found to be 900 GPa, I_b and I_c being the moment of inertia of the physical bolt shank and the cylindrical shell, respectively. This model is similar to the one proposed by Kwon *et al.* [**17**] except that instead of using the elastic modulus they changed the outer diameter, which resulted in a larger bolt hole.

5.4 Simplified model 4: rigid shell bolt

This is the same as model 3 except that the bolt–nut assembly is modelled using rigid shell elements. Because of the restraining effect of the bolt head and nut, the washers are assumed not to bend. The bolt shank is also assumed to be non-deformable. It is modelled as a rigid cylinder.

5.5 Simplified model 5: Timoshenko beam with coupling constraints

In this simplified model, the bolt shaft is modelled with a Timoshenko beam, B32, a three-node quadratic beam element. This type of beam accounts for the effects of the shear stress, which makes it suitable for application to short beams such as bolt shanks. The two nodes at the tips of the beam are chosen as the control points for the coupling constraints that restrain the relative motion between the ends of the beam and the region of the plate or frame which is in contact with the washer, as shown in Fig. 7. These constraints simulate the effects of the clamping pressure of the bolt head and nut. In this model, only contact pairs 1 and 2, which are between the frame and the plate, and between the plate and the impactor, are introduced; no contact relation is considered between the bolt shank and the holes. This model resembles the model proposed by Kim *et al.* [**16**]; but the sheets are discretized using shell elements in the present model rather than brick elements and the beam element accounts for shear deformation in addition to bending, tension, and torsion.

5.6 Simplified model 6: Timoshenko beam with coupling constraints without a hole

In this model, the frame and the plate do not have bolt holes (Fig. 8). All the other features of the model are the same as in the previous case. Ignoring the holes reduces the complexity in the modelling of the sheets. In addition, the existence of material rather than holes may simulate the effect of contact between the bolt shank and the perimeter of holes.

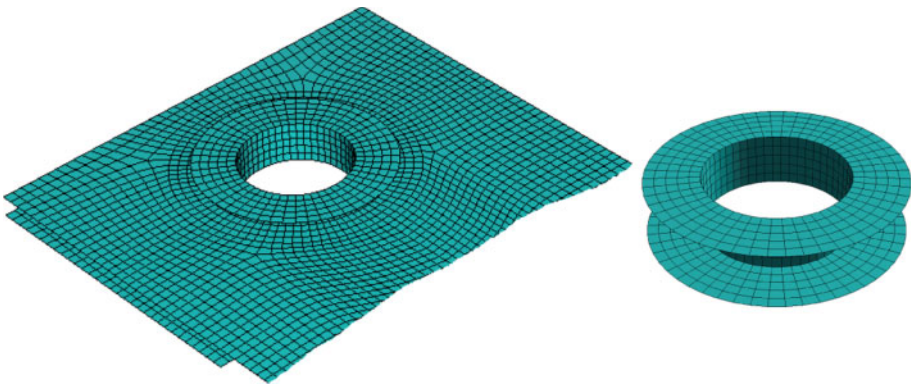

Fig. 6 Simplified model 3: deformable shell bolt

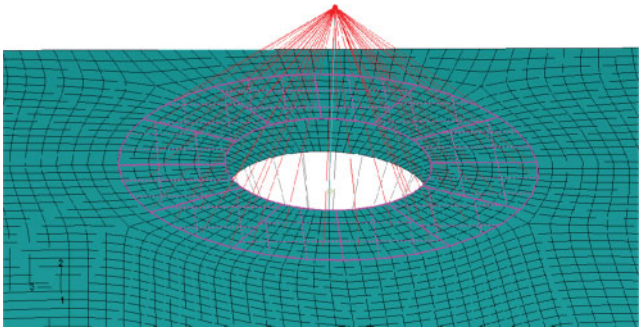

Fig. 7 Simplified model 5: Timoshenko beam with coupling constraints

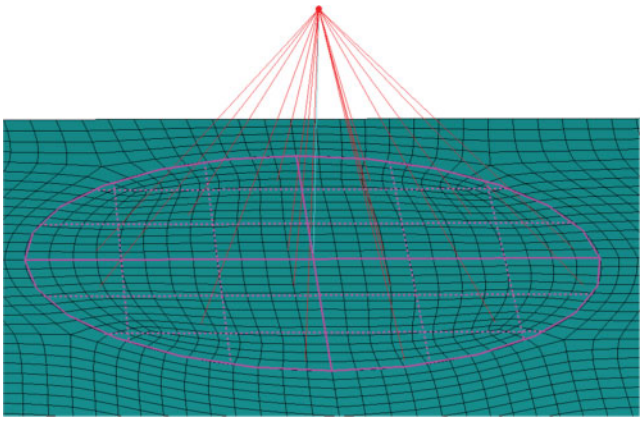

Fig. 8 Simplified model 6: Timoshenko beam with coupling constraints without a hole

5.7 Simplified model 7: tie constraint with hole

In this model, force transfer between the frame and the plate is achieved through a tie constraint defined between the inner surfaces of the sheets in the region compressed by the washers (Fig. 9). Tie constraints can be used to make the translational and rotational motions in all degrees of freedom the same for two surfaces.

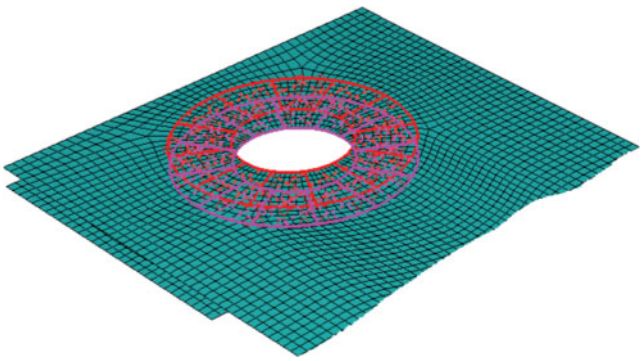

Fig. 9 Simplified model 7: tie constraint with hole

5.8 Simplified model 8: tie constraint withou a hole

This model also uses a tie constraint in order to model the clamping effect of the bolt–nut assembly as in the previous case; but there is no hole in this case. The relative distance between the plate and the frame in this region is thus kept constant during the impact via this constraint.

5.9 Simplified model 9: cross-coupling constraint

In this model, a kinematic coupling constraint is used to simulate the force transmission between the sheets (Fig. 10). A control point is defined at the centre of the bolt hole. All degrees of freedom at the nodes on the surfaces compressed by the washers are coupled with those of the control point. Only contact pairs 1 and 2 are introduced in this model.

5.10 Simplified model 10: connector beams along the perimeter of the hole

In this model, as can be seen in Fig. 11, 12 connector beam-type elements are defined, each element being

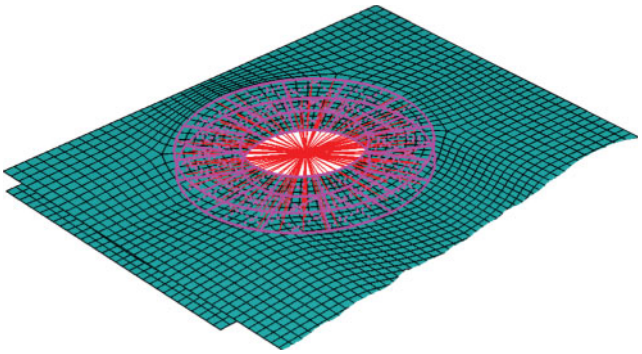

Fig. 10 Simplified model 9: cross-coupling constraint

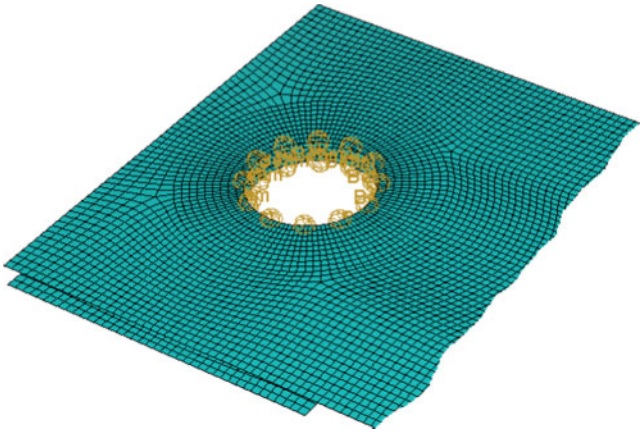

Fig. 11 Simplified model 10: connector beams along the perimeter of the hole

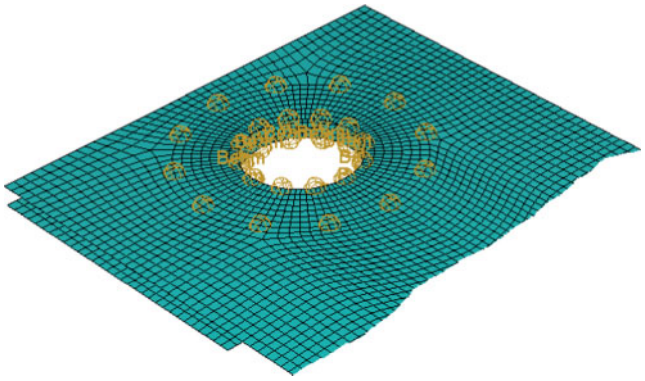

Fig. 12 Simplified model 11: connector beams along the perimeter of the hole and the washer's outer profile

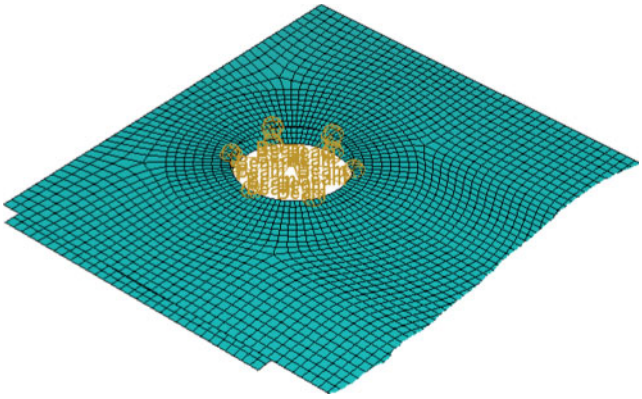

Fig. 13 Simplified model 12: cross connector beams

between the corresponding nodes of the plate and the frame to create a rigid connection between the two sheets. They are positioned on the perimeters of the bolt holes. Assuming the bolt–nut assembly to be non-deformable, relative motion between the sheets may be assumed to be completely prevented through the clamping pressure of the bolted joint. Accordingly, rigid connectors prevent relative motion between the plate and the frame at the perimeters.

5.11 Simplified model 11: connector beams along the perimeter of the hole and the washer's outer profile

The only difference between this model and the previous one is the additional restrained circular region. Twelve more connector beam elements are used to connect the frame and the plate along the projection of the outer edge of the washers (Fig. 12). In this way relative motion is prevented at extra points in the compressed region.

5.12 Simplified model 12: cross connector beams

In this model, there are 12 connector beam-type elements that join the midpoint of the line between the centres of the holes and nodes at the perimeters. Six of the connector elements are connected to the plate and the other six are connected to the frame (Fig. 13). Only the contact pairs 1 and 2 are introduced in this model.

6 RESULTS AND DISCUSSION

6.1 Validation of the solution

Because the finite element method is an approximate solution technique, one should ensure that the resulting error is less than an acceptable limit. The finite element software guides the user by issuing some warning messages for certain mistakes that the user can make in the modelling; but one should not solely rely on these messages. One of the ways to check the accuracy of the results is to use mesh-convergence analysis. One should determine the range of values for the mesh size for which one can obtain consistent results. Energy output is another indicator for the validity of the results of an explicit analysis. Based on comparisons between various energy components one may decide whether an analysis has yielded acceptable results.

6.1.1 Examination of the energy outputs

The energy balance for the entire system can be written as

$$E_{\mathrm{I}} + E_{\mathrm{K}} - (E_{\mathrm{W}} - E_{\mathrm{FD}} - E_{\mathrm{VD}}) = \text{constant} \tag{2}$$

where E_{I} is the internal energy, E_{K} is the kinetic energy, E_{W} is the work done on the structure by the externally applied loads, E_{FD} is the frictional energy dissipated, and E_{VD} is the viscous energy dissipated. The internal energy, E_{I}, is the sum of the recoverable elastic strain energy, E_{E}, the energy dissipated through inelastic processes such as plasticity, E_{P}, the energy dissipated through viscoelasticity or creep, E_{CD}, and the artificial strain energy, E_{A}

$$E_{\mathrm{I}} = E_{\mathrm{E}} + E_{\mathrm{P}} + E_{\mathrm{CD}} + E_{\mathrm{A}} \tag{3}$$

The artificial strain energy is introduced into the numerical model to constrain the hourglass deformation modes; therefore it is not associated with real deformation modes. Large values of the artificial energy mean that a significant portion of the impact

energy is used to stabilize the computational process rather than to simulate the physical process. In that case, improvement in the mesh is required. As an additional requirement the resultant sum of these energy components, given in equation (2) for the entire system, should remain constant.

First, the energy histories of the full model were examined. These are shown in Fig. 14. At the beginning of the simulation the impactor is in free fall, and all the energy is in the form of kinetic energy. During the initial stages of impact, mechanical energy is transferred to the plate, resulting in deformation of the sheets, with an increase in the internal energy and reduction in the kinetic energy. The sheets then deflect until the middle of the plate reaches its maximum deflection. After that the impactor recoils leading to an increased kinetic energy. Because the impact load is severe, energy expended on plastic deformation constitutes a significant portion of the internal energy. As seen in Fig. 14, the artificial energy of the system remains a small fraction of the internal energy and the total energy remains almost constant during the simulation. The energy histories of the simplified modes were also examined and they were found to be acceptable.

6.1.2 *Convergence analysis for the full model*

Convergence analyses were conducted for the full bolt model and the simplified models to determine a suitable element size. The maximum equivalent plastic strain and equivalent stress around the bolt hole and the maximum deflection were chosen as the control parameters. In the convergence analysis,

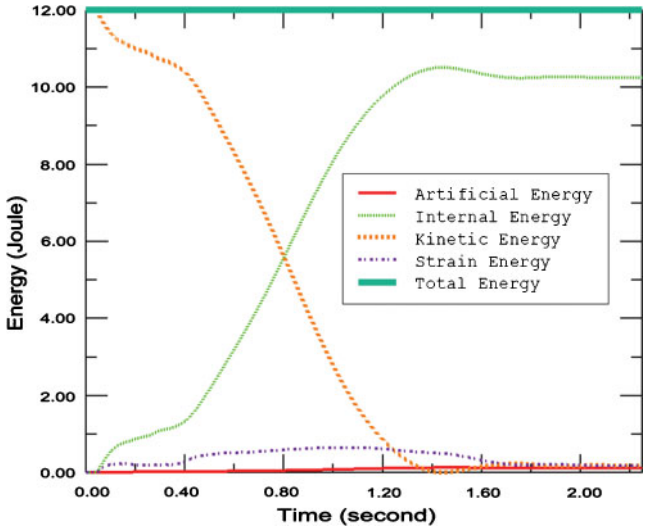

Fig. 14 Energy results versus time for the full model

the chosen element sizes were 2.0, 1.0, 0.66, and 0.5 mm; the dimensions of the brick elements in the thickness direction were equal to half of these values. Accordingly, in the full model, there were one, two, three, and four elements through the thickness of the plate corresponding to mesh sizes of 2.0, 1.0, 0.66, and 0.5 mm, respectively. Table 1 presents the results for the full model without including the pre-tension. The poor performance of the model with a mesh size of 2.0 mm can be attributed to the use of a single element through the thickness. However, for finite element sizes less than 1.0 mm, the model gives consistent results. After carrying out convergence analyses at different speeds and in other locations, the mesh size to be used in the comparisons was chosen as 0.66 mm. Table 2 presents the results for the full model with the effect of the pre-tension included. A temperature difference is introduced to the washer that induces expansion causing tension in the bolt shank that is equal to 80 per cent of the yield strength, which is 220 MPa. The results show a decrease in the plastic strains near the bolt as expected; however, the stresses around the bolt hole are almost the same. A slight decrease also occurs in the central displacement. The pre-tension makes the joint stronger and ignoring its effect leads to somewhat conservative results; however, since the pre-tension is not accounted for in the simplified models, comparison of the simplified models is made with the full model that does not consider the pre-tension.

Because, the sheets are modelled as shell structures in the simplified models, in which a single element exists through the thickness, convergence can be achieved at a larger element size; but comparisons are made using the same element size as that of the full model. For that reason, the gain obtained in the computational time will be due to the simplification in the model not due to a coarse mesh.

6.2 Comparison of the results of the simplified models and the full model

Table 3 gives a comparison of the results obtained using the simplified models and the full model regarding the maximum equivalent stress and plastic strain at two different locations and the central deflection of the plate. The stress and strain values are compared around the perimeter of the bolt hole and in the inner regions of the plate between the frame and the impactor. The values are normalized

Table 1 The results of the convergence analysis for the full model without the pre-tension

Mesh size (mm)	Equivalent stress around the hole (MPa)	Plastic strain around hole	Central displacement (mm)	Analysis time (s)
2.0	431	0.0398	−13.42	247
1.0	452	0.0964	−15.13	2448
0.66	458	0.1006	−14.99	18 735
0.5	460	0.1139	−15.14	59 183

Table 2 The results of the convergence analysis for the full model with the pre-tension

Mesh size (mm)	Equivalent stress around the hole (MPa)	Plastic strain around hole	Central displacement (mm)
2.0	396	0.0326	−13.04
1.0	442	0.0623	−14.32
0.66	450	0.0855	−14.53
0.5	457	0.0899	−14.62

such that the values of the full model are equal to 100. The saving in the computational time achieved through the use of the simplified models is about 80–90 per cent except for the first case. The simplified bolt models 10 and 12 highly overestimate the plastic strain at the perimeter of the bolt holes. Models 2, 5, 6, 7, 8, and 9 highly underestimate the plastic strain at the perimeter, whereas they highly overestimate in the inner region. Considering that the total kinetic energy transferred to the structure is the same for each case and it is largely transformed into strain energy for plastic deformation, it is understandable that if a model highly overestimates the deformation at one location it is likely that it underestimates the deformation level at other locations. The performances of simplified models 10, 11, and 12, which have local connections around the perimeter, depend on the mesh density. If the mesh density of the sheets is increased, strain and stress increase due to localization effects. In that case, the number of local connections should be increased to relieve stress concentration; but then the models become impracticable with a high number of connections. For the chosen mesh density, their performance is poor as seen in Table 3; but they yield acceptable results with a coarse mesh.

Comparisons were also made at a different impact speed (5 m/s). For the two speeds, the results indicate that simplified model 3, deformable shell bolt (Fig. 6), represents the full model best. Although the rigid shell bolt yields less accurate results than the deformable one, it is better in terms of modelling difficulty and computational time. Figures 15 to 17 show the equivalent stress distribution in the plate and its deformation state at its maximum deflection for the full model and simplified models 3 and 4, respectively. The reason why these models are more successful in representing the behaviour of the bolted joints is that at high impact loads direct contact occurs between bolt shank and the sheets. Due to this contact significant stresses develop. Only models 1, 3, and 4 account for this effect. Although this contact is defined in model 2, the rigid connection between the bolt and the sheets results in no contact occurring during the simulations. The others take into account only the clamping effect, but not the contact between the bolt and the sheets. For this reason they fail to reflect the impact response of the joint; but they better simulate the response at low impact loads.

Table 3 Normalized values of the chosen outputs of the bolt models

The model	Analysis time (s)	Plastic strain around the hole	von Mises stress around the hole	Plastic strain in the inner zone	von Mises stress in the inner zone	Central displacement
Full model	100.0	100.0	100.0	100.0	100.0	100.0
S.M. 1	73.4	86.2	100.4	174.9	106.6	97.9
S.M. 2	16.5	48.8	93.4	773.5	99.5	86.7
S.M. 3	13.0	94.8	102	154.2	108.2	99.9
S.M. 4	11.8	89.0	101.8	228.9	108.4	82.6
S.M. 5	15.2	47.6	91.8	745.2	101.9	86.8
S.M. 6	16.2	50.8	95.0	822.6	97.8	86.2
S.M. 7	14.3	56.8	96.6	1120.3	101.6	85.9
S.M. 8	15.8	62.8	97.0	1048.2	101.6	85.5
S.M. 9	14.5	47.0	96.6	1069.4	101.7	85.3
S.M. 10	15.4	933.1	274.7	157.0	102.2	98.7
S.M. 11	12.6	133.4	104.5	979.2	102.4	86.8
S.M. 12	14.5	894.1	125.0	272.3	99.5	95.0

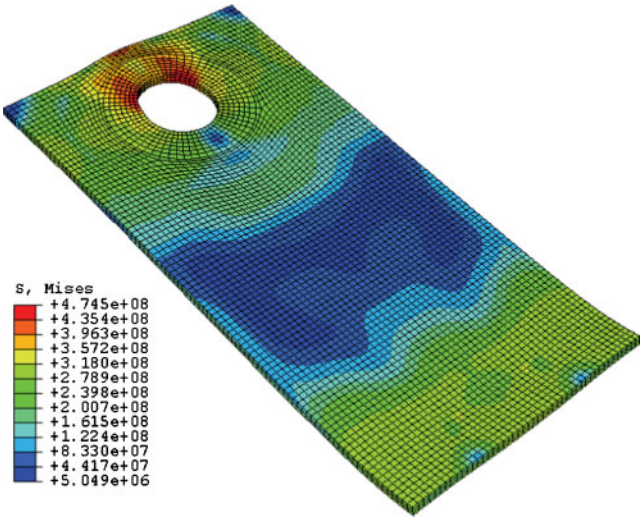

Fig. 15 Deformation state and equivalent stress state of the plate at the maximum deflection for the full model

7 CONCLUSIONS

Development of accurate and computationally efficient finite element models of bolted joints under impact loading was the goal of this study. In order to accurately determine the response of the structure, a detailed model was developed that accounted for almost all of the factors that influenced the stress and strain states in the joined sheets. In order to determine the structural response at a minimal computational burden, a number of simplified models were developed. The full model was then used as a benchmark for the accuracy of the simplified models.

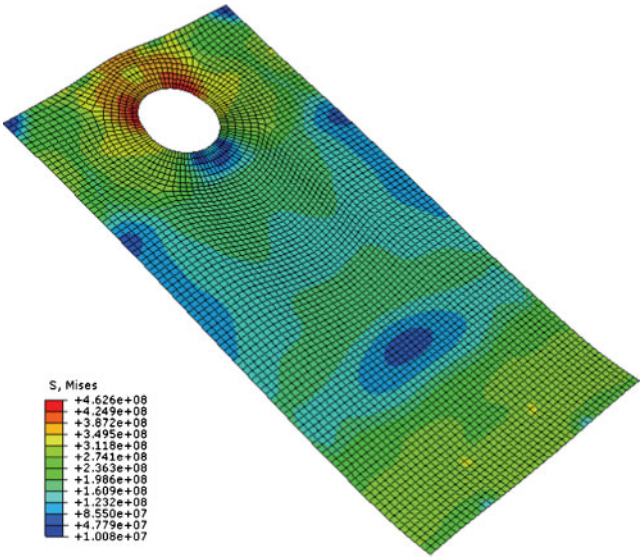

Fig. 16 Deformation state and equivalent stress state of the plate at the maximum deflection for simplified model 3

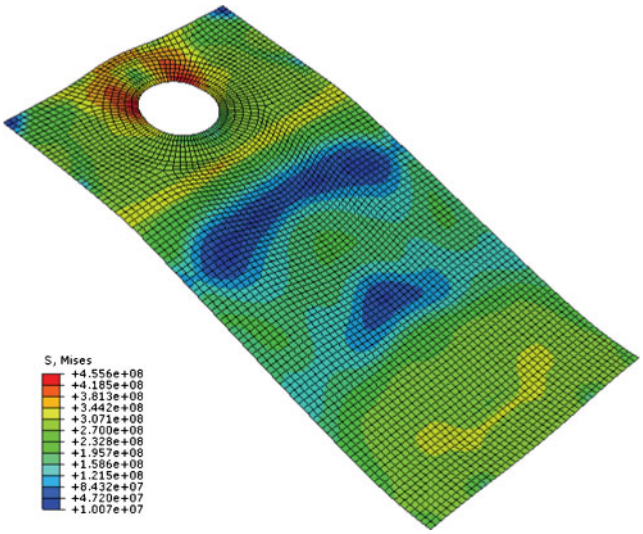

Fig. 17 Deformation state and equivalent stress state of the plate at the maximum deflection for simplified model 4

All of the simplified models, except simplified model 1, saved significant computational time when compared with the full model using the same mesh density. The saving in the computational time is about 80–90 per cent. Because the sheets are discretized with solid elements in the full model, many elements should be used through the thickness to obtain convergence, unlike the simplified models in which shell elements are used. For this reason, convergence of the simplified models can be obtained with coarser meshes. In view of that, actual savings in time are much larger in practice.

Among the simplified models, model 3 most accurately predicts the mechanical behaviour of the structure for different loading cases and mesh densities. Complexity of the geometry is also greatly reduced in the model.

ACKNOWLEDGEMENT

Platform R&D and TOFAS Turk Otomobil Fabrikasi are gratefully acknowledged for their support of this research.

REFERENCES

1 **Mistakidis, E. S.** and **Baniotopoulos, C. C.** Steel T-stub connections under static loading: an effective

2-D numerical model. *J. Construct. Steel Res.*, 1997, **44**, 51–67.

2 **Bursi, O. S.** and **Jaspart, J. P.** Benchmarks for modelling of bolted connections. *J. Construct. Steel Res.*, 1997, **43**, 17–42.

3 **Bursi, O. S.** and **Jaspart, J. P.** Calibration of a finite element model for isolated bolted end-plate steel connections. *J. Construct. Steel Res.*, 1997, **44**, 225–262.

4 **Bursi, O. S.** and **Jaspart, J. P.** Basic issues in the finite element simulation of extended end plate connections. *Comput. Struct.*, 1998, **69**, 361–382.

5 **Chung, K. F.** and **Ip, K. H.** Finite element modelling of bolted connections between cold formed steel strips and hot rolled steel plates under static shear loading. *Engng Struct.*, 2000, **22**, 1271–1284.

6 **Chung, K. F.** and **Ip, K. H.** Finite element investigation on the structural behaviour of cold-formed steel bolted connections. *Engng Struct.*, 2001, **23**, 1115–1125.

7 **Kishi, N., Ahmed, A.,** and **Yabuki, N.** Nonlinear finite element analysis of top- and seat- angle with double web angle connections. *Struct. Engng Mech.*, 2001, **12**, 201–214.

8 **Swanson, J. A., Kokan, D. S.,** and **Leon, R. T.** Advanced finite element modelling of bolted T-stub connection components. *J. Construct. Steel Res.*, 2002, **58**, 1015–1031.

9 **Barth, K. E., Orbison, J. G.,** and **Nukala, R.** Behaviour of steel tension members subjected to uniaxial loading. *J. Construct. Steel Res.*, 2002, **58**, 1103–1120.

10 **Citipitioglu, A. M., Haj-Ali, R. M.,** and **White, D. W.** Refined 3D finite element modelling of partially-restrained connections including slip. *J. Construct. Steel Res.*, 2002, **58**, 995–1013.

11 **Ju, S. H., Fan, C. Y.,** and **Wu, G. H.** Three-dimensional finite elements of steel bolted connections. *Engng Struct.*, 2004, **26**, 403–413.

12 **Yorgun, C., Dalci, S.,** and **Altay, G. A.** Finite element modelling of bolted steel connections designed by double channel. *Comput. Struct.*, 2004, **82**, 2563–2571.

13 **Webber, J. P. H., Graham, U.,** and **Wisnom, M. R.** Strain distributions around fasteners in laminated plates under biaxial in-plane loading. *J. Strain Anal. Engng Des.*, 1997, **32**(3), 167–174.

14 **Butterworth, J.** Finite element analysis of structural steelwork beam to column bolted connections, Report, University of Teesside, UK, 2003.

15 **McCarthy, M. A., McCarthy, C. T., Lawlor, V. P.,** and **Stanley, W. F.** Three-dimensional finite element analysis of single-bolt, single-lap composite bolted joints: part I - model development and validation. *Compos. Struct.*, 2005, **71**, 140–158.

16 **Kim, J., Yoon, J. C.,** and **Kang, B. S.** Finite element analysis and modelling of structure with bolted joints. *Appl. Math. Model.*, 2007, **31**, 895–911.

17 **Kwon, Y. D., Kwon, H. W., Hwangbo, J. H.,** and **Jang, S. H.** Finite element modelling for static and dynamic analysis of structures with bolted joint. *Key Engng Mater.*, 2006, **306–308**, 547–552.

18 **Sabuwala, T., Linzell, D.,** and **Krauthammer, T.** Finite element analysis of steel beam to column connections subjected to blast loads. *Int. J. Impact Engng*, 2005, **31**, 861–876.

19 **Reid, J. D.** and **Hiser, N. R.** Detailed modelling of bolted joints with slippage. *Finite Elem. Anal. Des.*, 2005, **41**, 547–562.

20 **Oldfield, M., Ouyang, H.,** and **Mottershead, J. E.** Simplified models of bolted joints under harmonic loading. *Comput. Struct.*, 2005, **84**, 25–33.

21 **Hendricks, B. F.** and **Wekezer, J. W.** Finite element modelling of G2 guardrail. *Transp. Res. Record*, 1996, **1528**, 130–137.

22 **O'Daniel, J. L., Koudela, K. L.,** and **Krauthammer, T.** Numerical simulation and validation of distributed impact events. *Int. J. Impact Engng*, 2005, **31**, 1013–1038.

23 **Harewood, F. J.** and **McHugh, P. E.** Comparison of the implicit and explicit finite element methods using crystal plasticity. *Comput. Mater. Sci.*, 2007, **39**, 481–494.